LATVIAN JOURNAL OF PHYSICS
AND TECHNICAL SCIENCES
2026, N 2

DOI: 10.2478/lpts-2026-0010

COMPARATIVE THERMAL ANALYSIS OF SLOTLESS AND SLOTTED PERMANENT MAGNET SYNCHRONOUS MOTOR

A. Silitis*, J. G. Jekabsons, L. Ribickis

Institute of Industrial Electronics,
Electrical Engineering and Energy,
Riga Technical University
12-K1 Azenes Str., Riga, LV-1048, LATVIA
*e-mail: armands.silitis@rtu.lv

The paper presents an extended comparative thermal analysis of slotless and slotted permanent magnet synchronous motors (PMSMs). To position the investigated motor topologies within modern drive system development, a brief classification-based background on slotless motors is included. Analytical lumped-parameter thermal models are derived to describe copper loss generation, temperature-dependent resistance, volumetric heat source implementation, and stator-to-ambient heat transfer. Three-dimensional thermal simulations performed in Autodesk Fusion are used to compare temperature fields and thermal gradients for both motor constructions under identical operating conditions. The results show that slotless PMSMs reach lower peak winding temperatures and exhibit a more uniform temperature distribution, primarily due to the absence of stator teeth and reduced internal thermal resistance. These findings support the application of slotless PMSMs in high-efficiency and high-reliability drive systems.

Keywords: *Heat transfer, lumped-parameter model, motor design, permanent magnet synchronous motor, slotless motors, thermal analysis.*

1. INTRODUCTION

Permanent Magnet Synchronous Motors (PMSMs) are extensively utilised across diverse sectors such as electric vehicles (EVs), robotics, industrial applications, and aerospace owing to their high efficiency, precision, favourable power-to-weight ratio, and consistent torque output. [1] Thermal phenomena critically influence the performance capabilities of these electric motors within traction and drive systems. The torque-speed dynamics of electric motors are contingent upon variables like armature/rotor resistance and stator resistance. An increase in the operating temperature of an electric motor of even 10 °C (corresponding to 283.15 Kelvin) can precipitate a reduction in the motor's service lifespan by as much as 50 % [2], [3]. Comparative analysis of the thermal impacts between conventional slotted PMSMs and their slotless counterparts reveals significant findings and potential advantages associated with the latter's utilisation, particularly in terms of thermal efficiency. This enhanced thermal performance in slotless PMSMs can be attributed to their distinct stator construction which contrasts with that of slotted PMSMs. Additionally, slotless PMSMs exhibit superior torque compared to slotted versions with equivalent specifications, largely due to the slotless design facilitating increased rotor space with independently positioned magnets, and the placement of windings that minimises the air gap and mitigates the resistive effects of air in slot gaps typical of standard slotted PMSM [4].

2. SLOTLESS MOTOR BACKGROUND AND CLASSIFICATION CONTEXT

Slotless motors are gaining popularity for their ability to enhance the smoothness of operation and provide consistent torque output while minimising irregular effects. This performance improvement is derived from modifying the rotor and stator designs. Slotless motor design employs the use of a smooth surface instead of traditional grooves, which eliminates air gaps. The coils are strategically placed to interact with an unvarying magnetic flux, generating a consistent force or torque. In contrast, conventional electric motors utilise grooves to form air gaps, allowing for the generation of a strong magnetic field using a smaller amount of magnetizing current. This concept is illustrated in Fig. 1.

For a slotless motor, the stator lamination sheets are obviously very simple when compared to a slotted motor, and the creation of the winding is simpler from a manufacturing point of view when placing it in the motor. This provides an opportunity to simplify the engine rebuilding process. The stator winding usually has more space, so it can be loaded with a higher current. Considering that there are no spatial limitations of the grooves, different winding variations are possible. Due to the larger effective air gap of the slotless motor, greater tolerances are possible for the rotor position and the sensitivity to the actual mechanical air gap is much less than that of a slotted motor [5], [6].

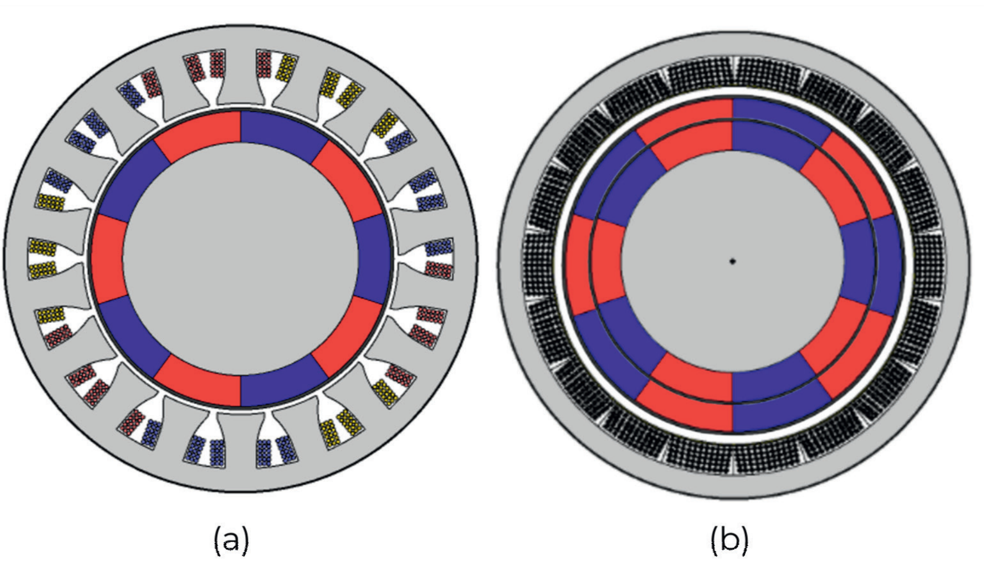

Fig. 1. Slotted (a) and slotless (b) PMSM 10 pole three-phase motor.

The design of slotless motors is based on permanent magnets – PM and stator specific windings (Fig. 2) so that the anchor winding does not have to supply current. If there is an increased air gap between the stator and armature windings, a stronger or larger PM would be needed, as the magnetic field intensity would decrease. The ribs have larger magnets and generally a larger rotor radius. The main advantage of the slotless motor design is that the lack of teeth in the lamination eliminates traction torque and creates a motor with very smooth operating parameters.

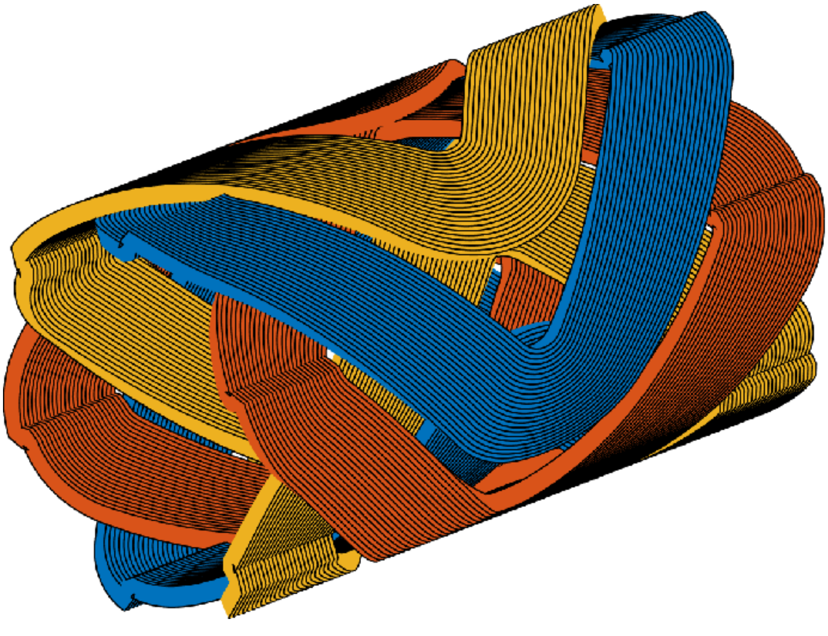

Fig. 2. 3-phase 6-coil slotless winding used as a basis [7].

3. THEORETICAL THERMAL MODELLING OF STATOR WINDINGS

The analytical estimation of stator winding temperature provides fundamental insight into the thermal behaviour of electric machines and serves as a validation reference for numerical simulations performed in Autodesk Fusion. In this study, a lumped-parameter thermal model is employed to compare the thermal performance of slotted and slotless Permanent Magnet Synchronous Motors.

3.1 Copper Loss Generation in Stator Windings

The applied heat power of 150 W corresponds to the total three-phase copper losses calculated under rated operating conditions. The copper losses were determined based on the rated phase current, phase resistance at operating temperature, and the effective winding volume. This approach ensures identical electrical loading conditions for both slotless and slotted PMSM models. The primary internal heat source in PMSMs during steady-state operation is copper loss generated in the stator windings. The total three-phase copper loss is expressed as:

$$P_{Cu} = 3I^2{}_{rms}R_{ph}(T_w), \quad (1)$$

where
P_{Cu} – total copper loss power (W);
I_{rms} – root-mean-square value of the phase current (A);
$R_{ph}(T_w)$ – phase resistance at winding temperature (T_w) (Ω).

This formulation assumes balanced three-phase sinusoidal currents and identical phase resistances, which is standard practice in PMSM thermal and loss modelling.

3.2 Temperature Dependence of Copper Resistance

Copper resistance increases approximately linearly with temperature:

$$R_{ph}(T_w) = R_{ph,ref}\left[1 + \alpha_{Cu}\left(T_w - T_{ref}\right)\right], \quad (2)$$

where
$R_{ph,ref}$ – phase resistance at reference temperature T_{ref} (Ω);
T_{ref} – reference temperature, typically 20 °C;
α_{Cu} – temperature coefficient of copper ($0.00393K^{-1}$);
T_w – winding temperature (°C).

This linear approximation is valid over the normal operating temperature range of electrical machines and is specified in IEC 60034-1.

3.3 Volumetric Heat Source for Simulation

In numerical thermal simulations, the copper loss is applied as a volumetric heat source distributed over the winding volume. The volumetric heat generation rate is given by Eq. (3):

$$q^{\cdot} = \frac{P_{Cu}}{V_w}, \quad (3)$$

where
$q^{\cdot}$ – the volumetric heat generation rate (W/m³);
V_w – the total copper winding volume (m³).

This heat source term is implemented in Fusion simulation as an input to the transient heat conduction equation (4):

$$\rho c_p \frac{\delta T_w}{\delta t} = \nabla \cdot (k \nabla T) + q,^{\cdot} \quad (4)$$

where
ρ – material density (kg/m³);
c_p – specific heat capacity (J/kg·K);
k – thermal conductivity (W/m·K);
T – local temperature field (K);
t – time (s).

3.4 Lumped Thermal Network Approximation

For engineering-level comparison, the distributed thermal field can be simplified using a lumped thermal RC network. The transient thermal behaviour of the winding is described by Eq. (5):

$$C_{th,w} \frac{dT_w}{dt} = P_{Cu} - \frac{T_w - T_s}{R_{th,(w-s)}}, \quad (5)$$

where
$C_{th,w}$ – thermal capacitance of the winding (J/K);
$C_{th,w}$ – thermal resistance between winding and stator surface (K/W);
T_s – stator surface temperature (°C).

This model captures the dominant heat storage and heat transfer mechanisms within the stator assembly.

3.5 Steady-State Winding Temperature

Under steady-state operating conditions, the time derivative term becomes zero, yielding Eq. (6):

$$T_{w,ss} = T_s + P_{Cu} R_{th(w-s)}. \quad (6)$$

This equation shows that the winding temperature rise above the stator surface temperature is directly proportional to copper losses and the internal thermal resistance.

3.6 Stator-to-Ambient Heat Transfer

Heat is dissipated from the stator surface to the surrounding environment primarily through convection. The stator surface temperature is therefore given by Eq. (7):

$$T_{s,ss} = T_{amb} + P_{Cu} R_{th(s-amb)}, \quad (7)$$

where
T_{amb} – ambient temperature (°C);
$R_{th(s-amb)}$ – thermal resistance between stator surface and ambient air (K/W).

The convection thermal resistance is expressed as Eq. (8):

$$R_{th,s-amb} = \frac{1}{hA_s}, \quad (8)$$

where
h – convection heat transfer coefficient (W/m²·K);
A_s – external stator surface area exposed to air (m²).

3.7 Final Expression for Steady-State Winding Temperature

By combining the previous expressions, the final steady-state winding temperature can be written as Eq. (9):

$$T_{w,ss} = T_{amb} + P_{Cu}(R_{th(w-s)} + R_{th(s-amb)}). \quad (9)$$

This formulation clearly demonstrates that the winding temperature is governed by both internal heat transfer (winding-to-stator) and external cooling conditions (stator-to-ambient). In slotless PMSMs, the absence of stator teeth and improved geometric uniformity reduce the thermal resistance resulting in lower winding temperatures compared to conventional slotted designs. This analytical conclusion is consistent with the numerical results obtained from Fusion simulations.

3.8 Simulation Assumptions

The thermal simulations were performed assuming identical operating conditions for both motor topologies. The ambient temperature was set to 25 °C. Radiative heat transfer was neglected due to its minor contribution at the considered temperature range. The winding copper losses were applied as a volumetric heat source of 150 W. The default adaptive mesh settings of Autodesk Fusion were used for all simulations.

4. THERMAL ANALYSIS OF SLOTLESS AND SLOTTED PMSMS

A 3D designated computational program Autodesk Fusion [8], [9] equipped with a simulation environment is employed to conduct thermal analyses and generate characteristic curves, thereby simulating the thermal distribution in both slotless and slotted PMSMs. For the purposes of simulation, three-dimensional models are constructed, reflecting the precise technical specifications of PMSM parameters and the materials used in their manufacture. The materials used in PMSM simulation are provided in Table 1 [10]. Convection boundary conditions were applied only to the external housing and stator outer surfaces exposed to ambient air. A natural convection heat transfer coefficient in the range of 25–33 W/m²·K was used. No convection was applied to the stator windings, where heat transfer was modelled exclusively by conduction.

Table 1. Thermal Conductivity of Materials Used in the Thermal Model

	Category	Material	Thermal conductivity (W/m·K)
1	Construction of the body	Steel	25.32
2	Stator	Silicon Steel	33
3	Stator windings	Copper	401
4	Slotless shell	Epoxy	1.02

Subsequently, the results, which vary according to the coefficient of thermal expansion specific to each material, are derived from each motor model. These results are documented and presented in Figs. 3–5.

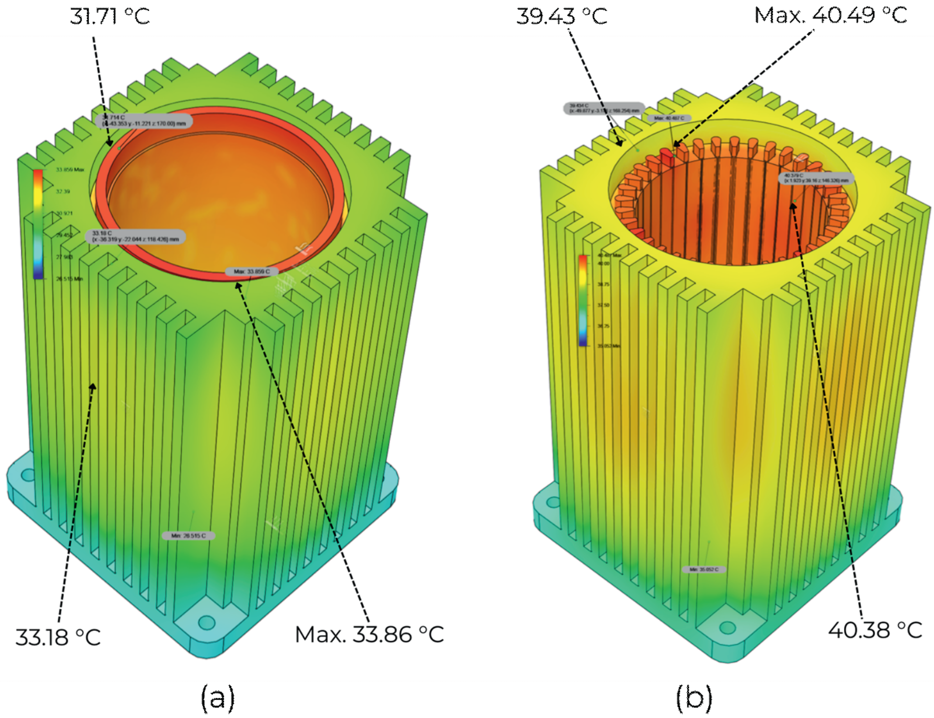

Fig. 3. Slotless (a) and Slotted (b) PMSM thermal simulation.

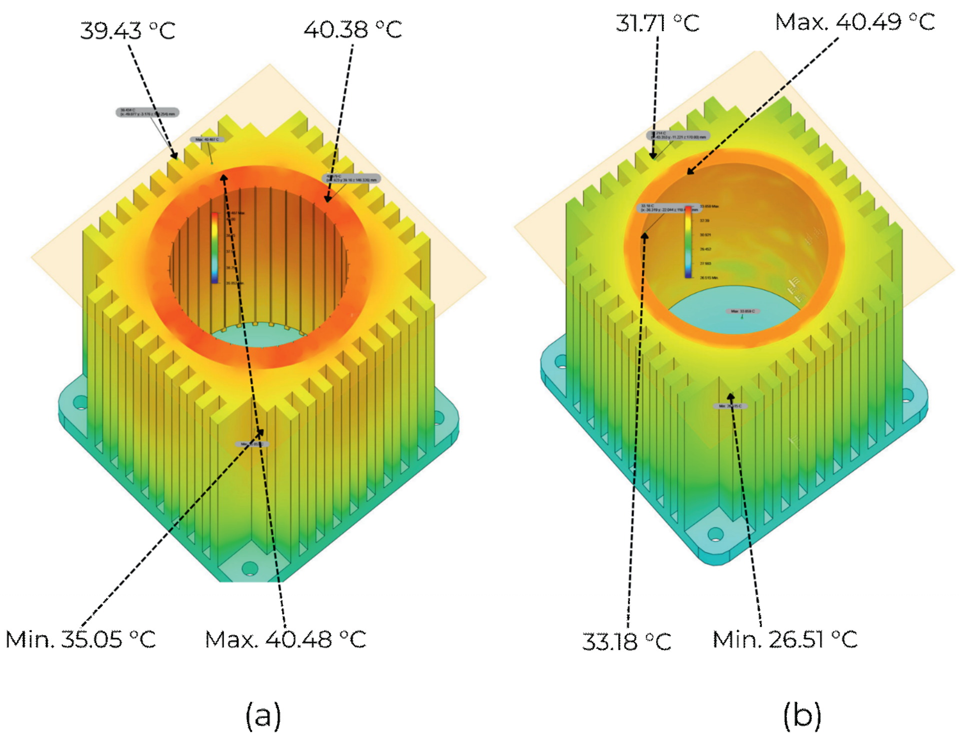

Fig. 4. Slotted (a) and Slotless (b) PMSM thermal simulation in cross-section.

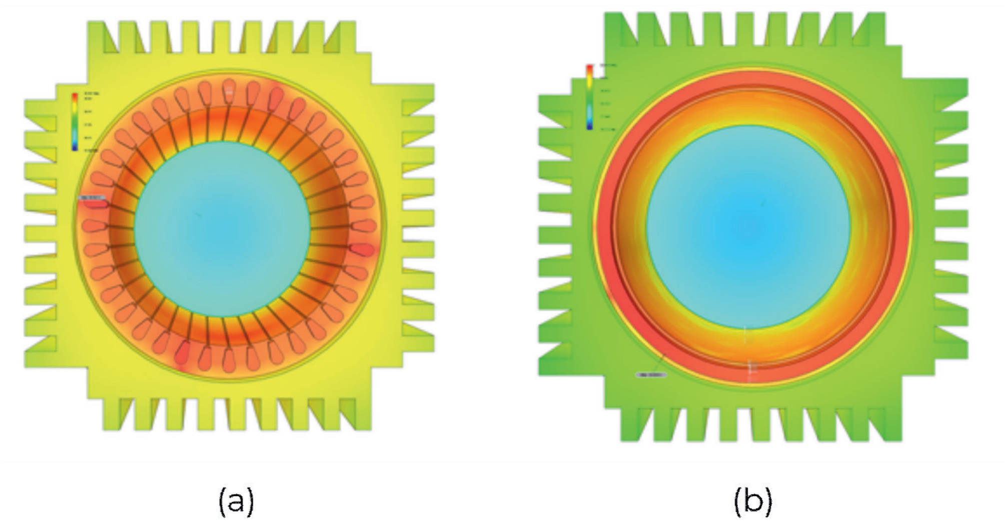

Fig. 5. Slotted (a) and Slotless (b) PMSM thermal convection.

5. RESULTS AND DISCUSSION

The empirical observations and computational visualisations presented here delineate the thermal gradients extant within slotted and slotless PMSMs amidst operational modalities.

The dataset accrued from the simulations of the median longitudinal cross-sections of the respective electric motors encapsulates the thermal dynamics incumbent in the heat dissipation processes pertaining to the motor housing, windings, and stator architecture. A discernible thermal increment of approximately 10 °C (equivalent to 283.15 Kelvin) (Figs. 4 and 5) was observed in the stator of slotted PMSMs in comparison with their slotless counterparts. This discrepancy is attributable to the geometric configurations of the stator slots, which ostensibly mitigate the effectiveness of thermal conductance back to the motor casing.

This thermal disparity can be explained by the intrinsic design of the stator within slotless motors. Herein, the windings are concentrically configured, devoid of the slots that in the slotted motors ostensibly act as thermal reservoirs, thus retaining elevated temperatures. Consequently, this distinct architectural paradigm significantly influences the thermal management efficiency of the respective motor types, with the slotless configuration exhibiting superior thermal performance characteristics.

6. CONCLUSIONS

In conclusion, the findings of this investigation provide robust validation for the hypothesis that slotless Permanent Magnet Synchronous Motors exhibit superior thermal performance relative to their slotted counterparts. This distinct advantage highlights the substantial potential for innovative design modifications within the realm of electric motor manufacturing, aimed at enhancing energy efficiency and operational reliability across a diverse spectrum of industrial and commercial applications. Furthermore, the research delineates a promising trajectory for future studies, emphasising the optimisation of motor designs that exploit these thermal benefits to augment overall motor efficacy. This study thereby contributes to the expanding body of knowledge within electromechanical engineering, promoting a deeper understanding of the thermal dynamics in motor technology and its implications for sustainable and efficient energy usage.

REFERENCES

1. Ali, S. M. N., Hanif, A., & Ahmed, Q. (2016). Review in thermal effects on the performance of electric motors. In *2016 International Conference on Intelligent Systems Engineering (ICISE)*, (pp. 83–88). Islamabad, Pakistan, 2016. https://doi.org/10.1109/INTELSE.2016.7475166
2. Bishop, T. (2004). Temperature monitoring is key to motor reliability: Regularly checking the operating temperature of each critical motor will pay dividends. *Maintenance Technology*, *17*, 34–37.
3. Tikadar, A. Kumar, N., Joshi, Y. & Kumar, S. (2020). *Coupled electro-thermal analysis of permanent magnet synchronous motor for electric vehicles*. Georgia Institute of Technology, Atlanta, GA, USA, 30332.
4. Bianchi, N., Bolognani, S., & Luise, F. (2005). Analysis and design of a PM brushless motor for high-speed operations. *IEEE Transactions on Energy Conversion, 20*(3), 629–637. https://doi.org/10.1109/TEC.2005.847991
5. Sīlītis, A. (2023). Analogy of slotless motor classification. In *2023 Asia-Pacific Conference on Image Processing, Electronics and Computers (IPEC 2023)*, Dalian, China, 14–16 April 2023. IEEE. https://doi.org/10.1109/IPEC57296.2023.00044
6. Bianchi, N., Bolognani, S., & Luise, F. (2006). High-speed drive using a slotless PM motor. *IEEE Transactions on Power Electronics, 21*(4), 1083–1090. https://doi.org/10.1109/TPEL.2006.876824
7. Burnand, G., Araujo, D. M., & Perriard, Y. (2018). Optimization of shape and topology for slotless windings in BLDC machines. In *Proceedings of the 21st International Conference on Electrical Machines and Systems (ICEMS),* (pp. 31–36). Jeju, Korea, 7–10 October 2018. https://doi.org/10.23919/ICEMS.2018.8549062
8. Autodesk. (n.d.). *Fusion 360* (product documentation). https://www.autodesk.com/products/fusion-360/overview
9. Song, P. P., Qi, Y. M., & Cai, D. C. (2018). Thermal modelling and simulation methods for electrical machines. *IOP Conference Series: Materials Science and Engineering, 359,* 012037. https://doi.org/10.1088/1757-899X/359/1/012037
10. Duong, M. T., Chun, Y. D., Park, B. G., Kim, D. J., Choi, J. H., & Han, P. W. (2017). Thermal analysis of a high-speed induction motor considering harmonic loss distribution. *Journal of Electrical Engineering & Technology, 12*(4), 1503–1510. https://doi.org/10.5370/JEET.2017.12.4.1503